Journal of Nano- and Electronic Physics
Vol. **16** No 4, 04010(5pp) (2024)

Журнал нано- та електронної фізики
Том **16** № 4, 04010(5cc) (2024)

OPEN ACCESS

REGULAR ARTICLE

Self-Isolated Dual L-Slotted 4-Port UWB MIMO Antenna with Wider Band-Notched Characteristics

T. Hemalatha, B. Roy* ✉

School of Electronics Engineering, VIT – AP University, Inavolu, 522237 India

(Received 20 April 2024; revised manuscript received 23 August 2024; published online 27 August 2024)

This research work addresses the challenges associated with isolation techniques in MIMO antenna design. The proposed 4-port L-Slotted Ultra-wideband (UWB) Multiple-Input Multiple-Output (MIMO) antenna design aims to offer a simple and compact solution that naturally ensures isolation between antenna elements. By employing innovative design strategies, notably incorporating L-Slotted structures, the research aims to extend the impedance bandwidth to 14.28 GHz, with a notch band covering the X-band and the lower portion of the Ku-band. The antenna's performance is evaluated by examining key metrics such as reflection coefficient (< – 10 dB), isolation (< – 20 dB), and diversity parameters. The proposed antenna achieved notable maximum $|S_{11}|$ of 22.77 dB at 6.945 GHz, a peak gain of 10.61 dBi, ECC < 0.0044, TARC < – 10 dB, and a diversity gain of approximately 9.999 dB. The wide impedance bandwidth and compatibility with various frequency bands make this antenna design adaptable to diverse applications and environments, providing flexibility for different system requirements. With its compact and efficient design, this antenna can be integrated into Internet of Things (IoT) devices and smart appliances, enabling reliable and high-speed wireless connectivity. Wide impedance bandwidth makes this antenna design suitable for various wireless communication applications, including Wi-Fi, 5G, and beyond.

Keywords: Self-isolation, UWB, MIMO, L-Slot, Notch band, Rectangular patch.

DOI: 10.21272/jnep.16(4).04010 PACS number: 84.40.Ba

1. INTRODUCTION

In recent decades, Multiple Input Multiple Output (MIMO) technology has significantly transformed wireless communication systems, enabling significant advancements in capacity, reliability, and spectral efficiency [1]. The performance of MIMO systems is significantly influenced by the effects of mutual coupling. To confront this challenge, a variety of techniques have been developed to provide feasible solutions. Among these techniques, spatial diversity method [2] has proven effective in mitigating the impact of mutual coupling. The mixed coupling phenomena is made up of two components: the inductive coupling that arises from the circulating current between the leg to the arm, and the capacitive coupling that is made possible by the electric field between closely spaced arms [3]. This synergistic combination enhances the robust isolation among the antenna elements. A self-isolated MIMO antenna system working in the 3.4 – 3.6 GHz frequency range is described in [4], which is intended for 5G applications. The antenna system has dimensions of $150 \times 75 \times 7$ mm^3. It has a – 22 dB minimum isolation level and an ECC of less than 0.0004. In this setup, there is a 20.8 mm gap between antenna elements. Other methods include self-multipath [6] to obtain wideband decoupling with multiple transmission zeros, linked co-planar waveguide [5], spatial [7], and polarization diversity [8], inter-element spacing ($\lambda + 0.5$ mm, $\lambda + 2.5$ mm, $\lambda - 2.5$ mm) [9], rectangular stub in the partial ground [10], coupled CPW transmission lines [11], dual-layer superstrate structure [12], L-shaped slots [13], self-control by providing $\lambda/2$ to $\lambda/8$ spacing between the radiating elements [14], U-shaped slotted ground plane [15] enhanced the isolation between the radiating elements. The primary drawback of these techniques is their complexity and the subsequent increase in footprint as the number of antenna elements grows.

This research article introduces a simple, compact, and self-isolated 'L' shaped slotted ultra-wideband MIMO antenna with notch-band features. By leveraging the self-isolation feature, the design complexity is significantly reduced, enhancing the ease of implementation.

2. PROPOSED ANTENNA DESIGN

The design evolution, complete structure, featuring dimensional specifications, of the final 4-port The UWB-MIMO antenna configuration is illustrated in Fig. 1, with optimized parameter values tabulated in Table 1.

* Correspondence e-mail: bappadittya.roy@vitap.ac.in

Cite this article as: T. Hemalatha et al., *J. Nano- Electron. Phys.* 16 No 4, 04010 (2024) https://doi.org/10.21272/jnep.16(4).04010

Table 1 – Measurements of the L-Slotted MIMO Antenna (in mm)

Parameter	Dimensions (mm)	Parameter	Dimensions (mm)
L_s	40	S_2	4
W_s	40	S_3	3.3
L_g	16	S_4	3.3
W_g	4	L_1	5.5
L_p	15	L_2	5.5
W_p	10	G_1	5
L_f	5	G_2	5
W_f	4	G_3	4
S_1	4	S_w	0.7

The overall physical volume of the proposed design is $40 \times 40 \times 1.6$ mm^3 and is fabricated on an FR-4 material, characterized by a dielectric constant (ε_r) of 4.4, a thickness measuring 1.6 mm, and a loss tangent (tan δ) of 0.02. The MIMO antenna configuration is detailed herein. The four rectangular shaped radiating elements, as depicted in Fig. 1(a) (considered as reference antenna) are strategically positioned in orthogonal orientations to one another, ensuring ample spacing between the patch elements.

This deliberate configuration is aimed at effectively reducing interference while enhancing the performance of the antenna system. To achieve this, the entire ground plane of the reference antenna is modified to a partial ground plane configuration, as shown in Fig. 1(b). Furthermore, an 'L'-shaped slot is incorporated into the lower right corner of the radiating portion, as portrayed in Fig. 1(c). Subsequently, another L-shaped slot is introduced at the opposite corner of the patch, as demonstrated in Fig. 1(d). Detailed analysis of the simulated results is provided in the subsequent section.

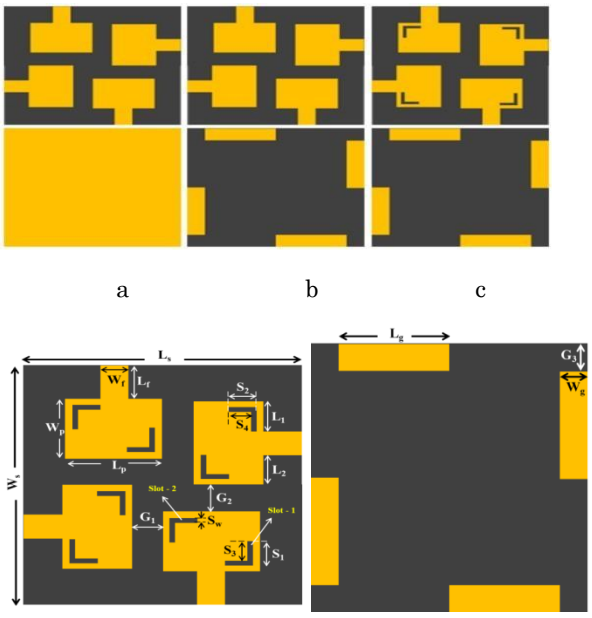

Fig. 1 – Design evolution of L-Slotted UWB MIMO

3. RESULTS AND DISCUSSION

The performance evaluation of the proposed L- Slotted ultra-wideband MIMO antenna design was conducted using HFSS 2021 R2 software. The reflection coefficient was analyzed at various stages of the design evolution, and the outcomes are illustrated in Fig. 2.

Initially, in Fig. 1(a), the MIMO antenna resonated at higher frequencies. Following the alteration of the ground, as presented in Fig. 1(b), the antenna resonated at lower frequencies, achieving an impedance bandwidth of 5.22 GHz (10.2 – 15.42 GHz). Further enhancement was attained with the introduction of the 'L'-shaped slot (slot-1) at the lower right corner of each radiating element, as represented in Fig. 1(c). This modification extended the impedance bandwidth ($S_{11} < -10$ dB) to 13.7 GHz (5.06 – 18.76 GHz).

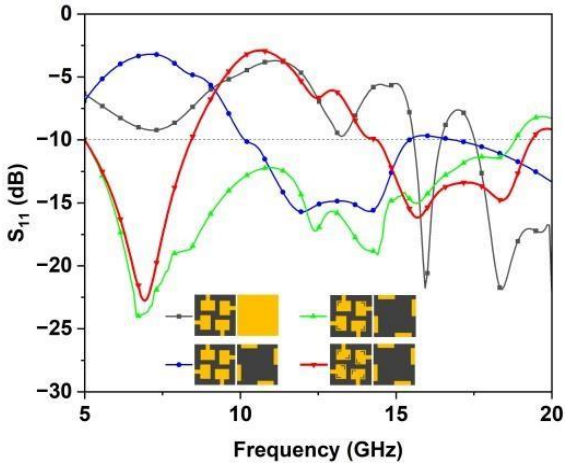

Fig. 2 – S_{11} (dB) at various stages of design evolution

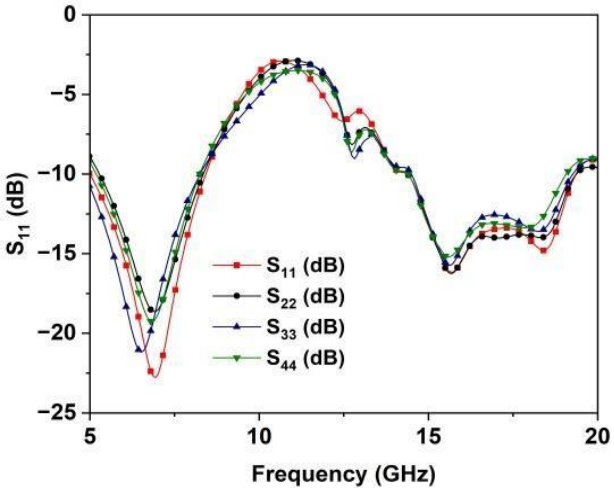

Fig. 3 – S-Parameters of the UWB MIMO Design

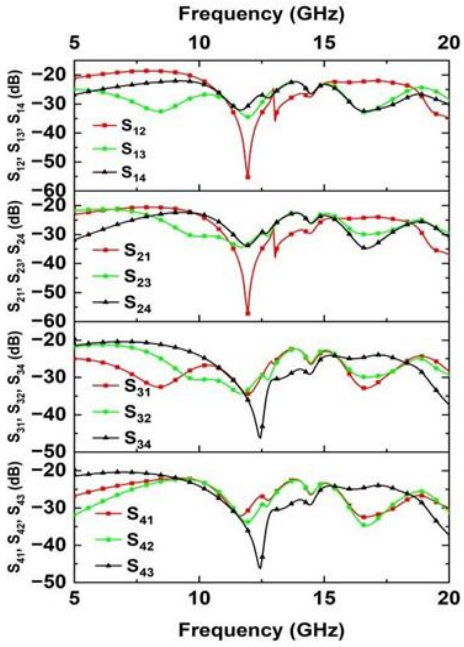

Fig. 4 – Isolation (dB) vs. Frequency (GHz)

Continuing the refinement process, as presented in Fig. 1(d), the UWB frequency coverage was augmented to 14.28 GHz (5.06 – 19.34 GHz). Notably, the addition of the second L-shaped slot (slot–2) acted as a $\lambda/2$ resonator, establishing a notch band with center frequency of 11.4 GHz. The reflection coefficient of all four radiating elements is illustrated in Fig. 3. Notably, a distinct notch band centered at 11.4 GHz is achieved, ranging from 8.39 to 14.41 GHz falls within the 'X'-band and lower end of 'Ku'-band and attained maximum $|S_{11}|$ of – 22.77 dB at 6.945 GHz frequency.

The key innovation of this study lies in its capacity to effectively resolve the isolation challenge while upholding high antenna efficiency. By leveraging inherent self-isolation properties using 5 mm distance between the orthogonal elements, the antenna has achieved robust isolation of over 20 dB (as depicted in Fig. 4) without resorting to additional decoupling elements or isolation techniques. Moreover, the proposed system presents a compact antenna size and a straightforward structure, thereby improving its practicality and ease of implementation. To demonstrate the effectiveness of the self-isolated antenna element within the MIMO system and its role in achieving satisfactory isolation, Fig.5 illustrates the surface current distribution of the antenna system at 6.945 GHz. Notably; the current intensity is primarily concentrated within the region bounded by the excited antenna area.

Fig. 6 illustrates the 2D radiation pattern at the resonant frequency of 6.945 GHz for orientations, $\varphi = 0°$ and $\varphi = 90°$. It is noteworthy that the proposed design exhibits its highest radiation power in the broadside direction. The plot presented in Fig. 7(a) illustrates a peak gain of 10.61 dBi, attained at a frequency of 6.43 GHz.

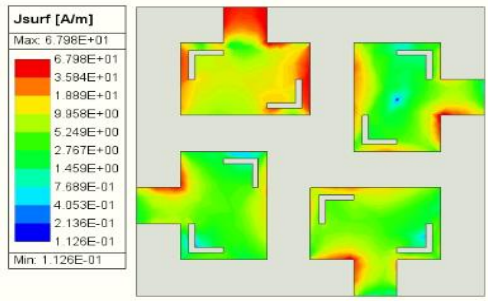

Fig. 5 – Surface current distribution at 6.945 GHz

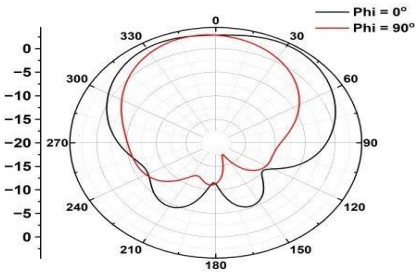

Fig. 6 – Radiation pattern at 6.945 GHz

Three important metrics related to diversity in MIMO systems are ECC (Envelope Correlation Coefficient), TARC (Total active reflection coefficient), and Diversity Gain.

The correlation coefficient quantifies the degree of correlation or isolation among multipath communication channels. ECC can be computed using far-field radiation patterns by means of Eq. (1) [16], achieved ECC < 0.0044 depicted in Fig. 7(b).

$$ECC = \frac{\left|\iint_{4\pi}[E_i(\theta,\phi) \times E_j(\theta,\phi)]d\Omega\right|^2}{\iint_{4\pi}|E_i(\theta,\phi)|^2 d\Omega \times \iint_{4\pi}|E_j(\theta,\phi)|^2 d\Omega} \quad (1)$$

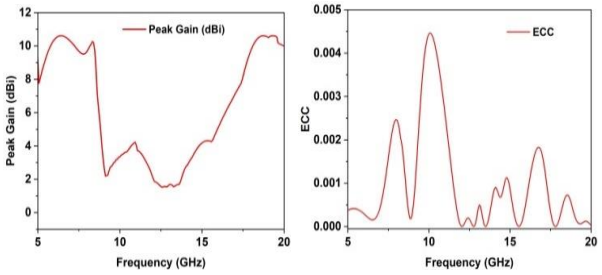

a b

Fig. 7 – (a) Peak Gain (dBi), (b) ECC

The TARC and diversity gain responses of the proposed structure is showcased in Fig. 8. With a TARC value below – 10 dB, the results indicate strong isolation between the radiating elements. Also achieved diversity gain ≅ 10 dB, calculated using Eq. (2) [17].

$$DG = 10 \cdot \sqrt{1 - (ECC)^2}$$

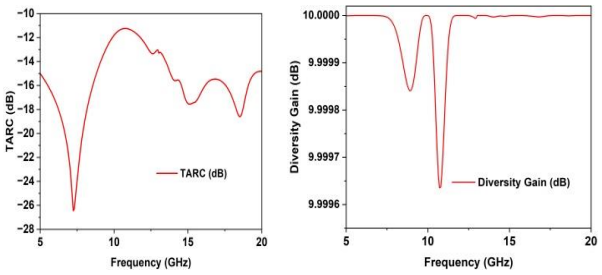

Fig 8 – (a) TARC (dB), (b) Diversity gain (dB)

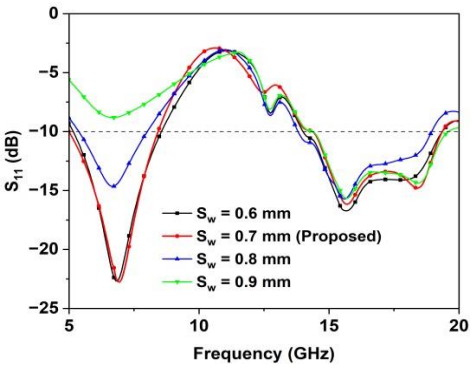

Fig. 9 – S_{11} (dB) for different slot-1 widths (S_w)

To conduct a parametric analysis, the S_{11} performance of the MIMO antenna was evaluated across four distinct slot-1 widths (S_w) and the attained outcomes depicted as Fig. 9. The investigation revealed that a slot-1 width of 0.7 mm yielded superior outcomes in terms of both S_{11} values and bandwidth characteristics. Fig. 10 depicts the fabricated prototype, showcasing both top and bottom views of the proposed L-Slotted rectangular patch UWB-MIMO antenna, alongside the measurement setup.

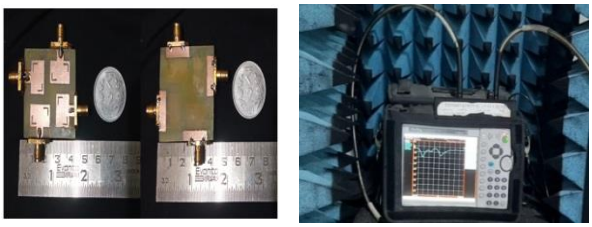

a b

Fig. 10 – (a) Fabricated Prototype, (b) Measurement setup

The comparison between simulated and measured outcomes of the proposed structure is displayed in Fig. 11, revealing a significant agreement. Furthermore, the antenna's performance is compared with conventional MIMO designs, with the results tabulated in Table 2. The comparative analysis demonstrates that the proposed simple MIMO design achieves high operational frequency coverage with a maximum peak gain of 10.61 dBi.

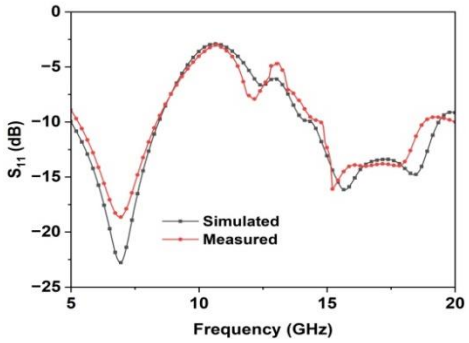

Fig. 11 – Reflection Coefficient - Sim. vs. Mea.

Table 2 – Comparative performance analysis of the proposed design with conventional antenna designs

Ref. No	Technique to enhance isolation	Dimensions (mm2)	Wideband range (GHz)	Bandwidth (GHz)	Peak gain (dBi)	ECC	No. of notch bands	Isolation
[3]	Capacitive and inductive coupling	125 × 70	3.29–3.66	0.37	–	< 0.175	–	> 20
[7]	20 mm spacing	60 × 60	2.2–3.5 4.8–6.2 7.8–9.8	> 2	5.5	< 0.0001	–	> 30
[8]	Polarization diversity	22 × 1	3.3–6	2.7	–	< 0.2	–	> 12
[9]	λ+0.5mm, λ+2.5mm, λ-2.5mm	43 × 25	37.2–39.86	2.66	4.25	–	–	> 24
[11]	*L*-shaped self- decoupling	80 × 80	3.3–3.8	0.5	–	< 0.006	–	> 20
[14]	$\lambda/2$ to $\lambda/8$ spacing	50 × 100	3.3–3.6	0.3	6.72	–	–	> 20
Proposed work	5 mm spacing between the antenna elements	40 × 40	5.06–19.34	14.28	10.61	< 0.0044	1	> 20

4. CONCLUSION

A simple, compact, low-complex L-Slotted UWB MIMO antenna was designed and developed that inherently achieved self-isolation between antenna elements. The proposed antenna design achieved the UWB of 14.28 GHz (5.06 GHz – 19.35 GHz) including the notch-band of 8.39 – 14.41 GHz (X-band and lower end of Ku-band). It also achieved the maximum $|S_{11}|$ of 22.77 dB at 6.945 GHz, peak gain of 10.61 dBi,

ECC < 0.0044, TARC < – 10 dB and diversity gain of ≅ 9.999 dB. The prototype's measured outcomes closely align with the simulated results, indicating a strong agreement between the two. Additionally, a comparative analysis of performance against traditional antennas was conducted and summarized in Table 2.

ACKNOWLEDGEMENT

The authors extend their gratitude to the Department of SENSE at VIT-AP University, RGEMS, and V-Launch Projects for their invaluable provision and inspiration during the course of this research endeavor.

REFERENCES

1. H. Wang, R. Zhang, Y. Luo, G. Yang, *IEEE Access* **8**, 19433 (2020).
2. El Hadri, Doae, Alia Zakriti, Asmaa Zugari, Mohssine El Ouahabi, Jamal El Aoufi., *Int. J. Antennas Propag.* **2020**, 2740920 (2020).
3. Singh, Harsh Verdhan, D. Venkata Siva Prasad, Shrivishal Tripathi, *Sci. Rep.* **13** No 1, 5636 (2023).
4. Hussain, Musa, Wahaj Abbas Awan, Mohammed S Alzaidi, Dalia H Elkamchouchi, *Heliyon* **9** No 7, e17404 (2023).
5. Z. Zhou, Y. Ge, J. Yuan, Z. Xu, Z.D.Chen, *IEEE Trans. Antennas Propag.* **71** No 2, 1414 (2023).
6. A. Zhang, K. Wei, Z. Zhang, *IEEE Trans. Antennas Propag.* **71** No 7, 5605 (2023).
7. F. Mohsenifard, A. Mahmoodzadeh, Z. Adelpour, *IEEE Access* **11**, 9483 (2023).
8. A. Ren, H. Yu, L. Yang, Z. Huang, Z. Zhang, Y. Liu, *IEEE Antennas Wireless Propag. Lett.* **22** No 7, 1642 (2023).
9. Fatima Kiouach, Mohammed El Ghzaoui, Samudrala Varakumari, et al., *J. Nano- Electron. Phys.* **15** No 1, 01025 (2023).
10. Singh, Ajit Kumar, Mahto, Santosh Kumar Sinha, Rashmi, *Frequenz* **77** No 3-4, 173 (2023).
11. Z. Zhou, Y. Ge, J. Yuan, Z. Xu, Z.D.Chen, *IEEE Trans. Antennas Propag.* **71** No 2, 1414 (2023).
12. Y. Li, Q.-X. Chu, *IEEE Antennas Wireless Propag. Lett.* **21** No 3, 521 (2022).
13. X. Yuan, et al., *IEEE Antennas Wireless Propag. Lett.* **23**, 99 (2023).
14. Salsanabila Mariestiara Putri, Indra Surjati, Syah Alam, et al., *J. Nano- Electron. Phys.* **15** No 6, 06007 (2023).
15. Sunandan Bhunia, Neha Gupta, Nitu Kumari, et al., *J. Nano- Electron. Phys.* **15** No 4, 04021 (2023).
16. T. Hemalatha, B. Roy, *AEU-Int. J. Electron. Commun.* **176**, 155118 (2024).
17. M. Sharma, A. Kumar, V. Kikan, et al., *Wireless Netw* **30**, 1815 (2024).

Самоізольована 4-портова UWB MIMO антена з подвійним *L*-прорізом і характеристиками ширшого діапазону

T. Hemalatha, B. Roy

School of Electronics Engineering, VIT – AP University, Inavolu, 522237 India

У цій дослідницькій роботі розглядаються проблеми, пов'язані з методами ізоляції в конструкції антен MIMO. Запропонована конструкція 4-портової надширокосмугової (UWB) антени з декількома входами та декількома виходами (MIMO) з *L*-щілинами має на меті запропонувати просте та компактне рішення, яке природно забезпечує ізоляцію між елементами антени. Застосовуючи інноваційні стратегії проектування, зокрема використовуючи структури з *L*-щілинами, дослідження спрямоване на розширення смуги пропускання імпедансу до 14,28 ГГц із смугою вирізів, що охоплює діапазон X і нижню частину діапазону Ku. Ефективність антени оцінюється шляхом вивчення ключових показників, таких як коефіцієнт відбиття (< – 10 дБ), ізоляція (< – 20 дБ) і параметри рознесення. Запропонована антена досягла помітного максимуму |S11| 22,77 дБ на 6,945 ГГц, пікове посилення 10,61 дБі, ECC < 0,0044, TARC < – 10 дБ і посилення рознесення приблизно 9,999 дБ. Широка смуга пропускання імпедансу та сумісність із різними діапазонами частот роблять цю конструкцію антени адаптованою до різноманітних додатків та середовищ, забезпечуючи гнучкість для різних системних вимог. Завдяки компактній та ефективній конструкції цю антену можна інтегрувати в пристрої Інтернету речей (IoT) і розумні пристрої, забезпечуючи надійне та високошвидкісне бездротове з'єднання. Широка смуга пропускання імпедансу робить цю конструкцію антени придатною для різноманітних програм бездротового зв'язку, включаючи Wi-Fi, 5G тощо.

Ключові слова: Самоізоляція, UWB, MIMO, *L*-слот, Насічна смуга, Прямокутний патч.